Original Article

Institution of MECHANICAL ENGINEERS
Journal of ENGINEERING IN MEDICINE

Proc IMechE Part H:
J Engineering in Medicine
2022, Vol. 236(1) 72–83

DOI: 10.1177/09544119211046675
journals.sagepub.com/home/pih
SAGE

On the hearing effects of a cholesteatoma growing: A biomechanical study

Leonor Mendonça[1,2], Carla F Santos[1,2], Fernanda Gentil[1,3], Marco Parente[1,2], Bruno Areias[1,2] and Renato Natal Jorge[1,2]

Abstract

Chronic otitis media enables the appearance of a benign middle ear tumor, known as a cholesteatoma, that may compromise hearing. To evaluate the influence of a cholesteatoma growth on the hearing function, a computational middle ear model based on the finite element method was used and three different size of cholesteatoma were modeled. The cholesteatoma solidification and the consequent degradation of the ossicles were also simulated as two condition that commonly occurs during cholesteatoma evolution. A sound pressure level of 80 dB SPL was applied in the tympanic membrane and a steady state analysis was performed for frequencies from 100 Hz to 10 kHz. The displacements of both the tympanic membrane and the stapes footplate were measured. The results were compared with a healthy case and it was shown that the cholesteatoma development leads to a decrease in the umbo and stapes displacements. The ossicles degradation simulation showed the higher difference comparing with the cholesteatoma in an initial stage, with lower displacements in the stapes footplate mainly for high frequencies. The observed displacement differences are directly connected to hearing loss, being possible to conclude that cholesteatoma evolution in the middle ear will lead to hearing problems, mainly in an advanced stage.

Keywords

Cholesteatoma, hearing loss, finite element method, growth simulation

Date received: 20 October 2020; accepted: 25 August 2021

Introduction

Hearing loss is considered to have a significant impact on the Global Burden of Disease, states the World Health Organization (WHO), which happens mainly in industrialized countries.[1]

Otitis media (OM) is an infection in the middle ear, being one of the most frequent conditions associated with human ear.[2] It can last 1 or 2 weeks, presenting intense pain and fluid in the middle ear cavity, known as acute otitis media. If it lasts for more than 3 months is considered chronic otitis media (COM), which could lead to hearing loss and cholesteatoma development. According to WHO, COM has a prevalence of around 1% in general population in developed countries.[3] A WHO study from 2017, which assessed the cost-effectiveness of preventive measures and interventions,[4] considered that hearing loss must be treated as a public health matter, due the 750–790 billion dollars estimation of the global cost associated with unaddressed hearing loss in the world. Thus, prevention and early diagnosis of ear diseases would be helpful to reduce these costs.

Cholesteatoma is the most frequent type of tumor that can result from COM, being a pouch like lesion composed of an accumulation of skin debris.[5] It can either be congenital or, in the majority of the cases, acquired.[6] Its development can happen due to Eustachian tube malfunction, since this way there is not a proper ventilation of the middle ear, hampering the

[1]INEGI, Institute of Mechanical Engineering and Industrial Management, Rua Dr. Roberto Frias, Porto, Portugal
[2]Faculty of Engineering of the University of Porto, Rua Dr. Roberto Frias, Porto, Portugal
[3]Clínica ORL-Dr. Eurico Almeida, Widex, Escola Superior de Saúde – I.P. Porto, Porto, Portugal

Corresponding author:
Carla F Santos, INEGI, Institute of Mechanical Engineering and Industrial Management, Rua Dr. Roberto Frias, Campus da FEUP, 400, Porto, 4200-465, Portugal.
Email: fsantos.carla@gmail.com

otitis treatment. Although this mass is usually a benign tumor, its surveillance is very important, since it can lead to the erosion of the nearby structures due to its expanding nature and surrounding inflammatory reaction.[7] This will release several molecules, namely lytic enzymes, cytokines, and growth factors that can recruit osteoclasts, capable of destroying bone cells.[6] Cholesteatomas can appear in several locations, interfering with the regular functions of the ear structures; mainly when it enlarges to engulf the underlying ossicles of the middle ear as it commonly lead to conductive hearing loss, due to bone chain erosion and degradation.[8] The mechanical structure of the middle ear chain losses its effectiveness in sound transmission due to osteoclast activation, pressure necrosis, acid lysis, inflammatory mediators, and some biomolecules.[9,10]

Moreover, a cholesteatoma that grows attached to the ossicles will also contribute to damping phenomena, leading to hearing loss, as there will be an extra mass that will affect sound transmission through the ossicles. The cholesteatoma properties also evolve along time, making it a harder and denser structure as it grows, increasing the damping phenomena.

It is estimated that cholesteatoma has an incidence of 9.2 per 100,000 habitants a year in northern Europe countries,[11] being higher in children from 5 to 15 years old. Men are more likely to develop acquired cholesteatoma, being the ratio men/women around 1.4.[6]

Lips et al.[7] studied cholesteatomas dimensions, concluding that their maximum diameter in transverse and coronal planes fluctuates between 4 and 27 mm, being the median value 9 mm. Some studies point out that although antibiotics treatment may be enough for a simple COM, when a cholesteatoma is present, there is the need of a surgery to remove the infected tissue and repair lesions that may have occurred.[6,7]

The finite element method (FEM) was used to conduct the current biomechanical study of the presence of a cholesteatoma in the middle ear. FEM simulations to study human ear conditions had been applied by several research groups in last decades, as Wang et al.[12] that created a three dimensional virtual model of the temporal bone to promote a better knowledge of this bone's anatomy among scientific community. Gan et al.[13,14] also had developed several research in the field, including the development of a detailed and complete model of the ear based on 780 histological sections of 20 μm thickness, including the external auditory canal, the cochlea, and ear fluids. This complete model allowed to obtain sound pressure gain, stapes and round windows movements, and the basilar membrane vibration. Other important research in the field is the work developed by Puria et al.[15] including the implications of otoacoustic emissions and the influence of mechanical properties in sound transmission.[16–18] Liu et al.[19] also performed relevant research in hearing field using FEM models as the work on the influence of the ossicular chain malformation on round window performance.

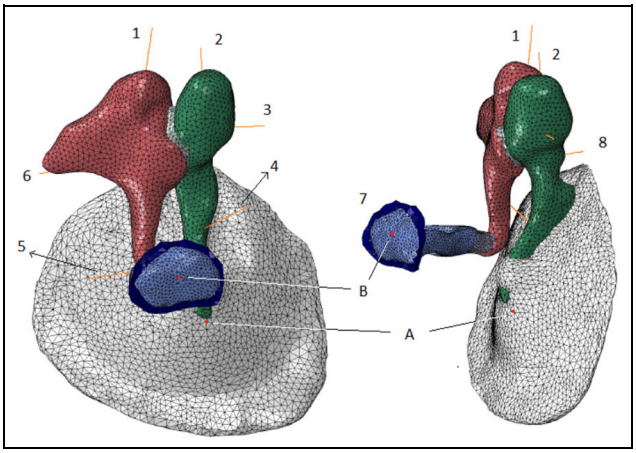

Figure 1. Finite element mesh of the middle ear structures, tympanic membrane (white), malleus (green), incus (pink), and stapes (blue). The other structures are: 1 – superior malleus ligament, 2 – superior incudal ligament, 3 – anterior malleus ligament, 4 – tensor tympani tendon, 5 – stapedius tendon, 6 – posterior incudal ligament, 7 – stapedius annular ligament, 8 – lateral malleus ligament, A – analysis node in the umbo, and B – analysis node in the stapes footplate.

Thus, the aim of the current work is to study the influence of cholesteatoma development on hearing function using a computational model.

Methods

Finite element model

The middle ear FEM model used in the present work was based in the project "The visible ear" of Sørensen et al.[20,21] The model, shown in Figure 1, is composed of the tympanic membrane, the ossicular bones (malleus, incus, and stapes), two tendons (stapedius tendon and tensor tympani tendon), six ligaments (superior malleus ligament, lateral malleus ligament, anterior malleus ligament, superior incudal ligament, posterior incudal ligament, and stapedius annular ligament), incudomalleolar joint (IMJ), and incudostapedial joint (ISJ). The tympanic membrane and the three ossicular bones have distinct properties for each part as detailed in Table 1. Femap (2019.1) and ABAQUS (Dassault Systemes. ABAQUS[22]) softwares were used in this work, being the first used to model the different structures and the latter to run the desired simulations.

The tendons and ligaments are simulated through truss elements of type T3D2 and the remaining parts of the ear with tetrahedral (C3D4) elements.

The appropriate boundary conditions were then applied. In the tympanic membrane, the tympanic sulcus allows for the connection with the bone. This was simulated by fixating the borders of the membrane. Inside the tympanic cavity, the malleus, the incus, and the stapes are connected to each other through the joints. In addition, they are hold by ligaments and muscles, which was simulated by connecting these

Table 1. Material properties of the FEM model.

Model component	Density(kgm^{-3})	Young's modulus (Nm^{-2})	Damping
Tympanic membrane	1.2×10^3	Pars tensa	$\alpha = 0\,s^{-1}$
		3.2×10^7 (radial)	$\beta = 0.0001$ s
		2.0×10^7 (circumferential)	
		Pars flaccida	
		1.0×10^7 (radial)	
		1.0×10^7 (circumferential)	
Malleus	2.55×10^3 (head)	1.41×10^{10}	
	4.53×10^3 (neck)		
	3.70×10^3 (handle)		
Incus	2.36×10^3 (body)		
	2.26×10^3 (short process)		
	5.08×10^3 (long process)		
Stapes	2.2×10^3		
Stapedius tendon	2.5×10^3		
Tensor tympani tendon	2.5×10^3		
Incudomalleolar joint	3.2×10^3	1.41×10^{10}	
Incudostapedial joint	1.2×10^3	6.0×10^5	
Superior malleus ligament	2.5×10^3	4.9×10^4	
Lateral malleus ligament		6.7×10^4	
Anterior malleus ligament		2.1×10^6	
Superior incudal ligament		4.9×10^4	
Posterior incudal ligament		6.5×10^5	
Stapedius annular ligament		2.0×10^4	

structures to the corresponding ossicle, in one end, and fixate it in the other, in order to mimic its connection to the tympanic cavity wall. Finally, the annular ligament connects the stapes to the bone, so it was also fixated. The bone was encastered in the extremities.

The mechanical properties used in the present model are based on the data available in the study of Sun et al.[23] and presented in Table 1. Poisson's ratio is assumed to be 0.3 for all parts of the human ear.[23] Rayleigh's proportional damping was introduced in the middle ear components, with the coefficients $\alpha = 0\,s^{-1}$ and $\beta = 0.0001$ s, equal to some other recent published models.[24,25]

Cholesteatoma simulation

In order to simulate a cholesteatoma growth, three different sized cholesteatomas were built and assembled to the middle ear model.[26] The chosen area for the cholesteatoma was the connection between the malleus and the incus, as this is typically the first spot for cholesteatoma accommodation.[8] The cholesteatomas were built with an ellipsoid shape, considering that the bigger one should be large enough to get close to the chorda tympani nerve (CTN), the facial nerve branch that crosses the middle ear. Although these tumors may also affect this nerve,[27,28] the focus of the current work was the effect of cholesteatoma development on hearing.

According to the values obtained by Lips et al.[7] the three cholesteatomas were built, being their dimensions and meshes information present in Table 2. The cholesteatomas volume was calculated through ABAQUS software.

The smaller cholesteatoma was the first to be created (Figure 2(c)). Regarding the dimensions mentioned in the Table 2, three diameters were measured, along three different axes. Diameter 1 concerns the vertical measurement, diameter 2 is measured in a perpendicular axis, being connected to the distance along the incudomalleolar joint, from the malleus to the incus, diameter 3 is in the same plan that diameter 2, but perpendicular to it, measuring the depth of the cholesteatoma. It is possible to see that this cholesteatoma dimensions are reduced, when comparing them to literature values. The cholesteatoma and its position in the middle ear are shown in Figure 2, being the three axes also evidenced. Figure 2(b) shows a cross section of the model with the small cholesteatoma in dark yellow (between the bones) and the light yellow elements represent the modified region considered as the ossicular degradation.

Next, the medium cholesteatoma was created. It was bigger than the first one, but not big enough to reach the CTN. Diameters 2 and 3 are, once again, slightly lower than reference values, as one can see in Table 2.

Finally, the third cholesteatoma was created. This was the larger one. This cholesteatoma dimensions are closer to the acceptable values described in literature. The larger cholesteatoma was designed considering that it should be able to reach CTN and wrap it.

Initially, the three cholesteatomas were considered to have similar properties. As the literature is scarce regarding that matter, and considering the cholesteatoma is defined as "accumulation of skin debris" considered a benign tumor, the authors assume the properties of cancerous skin to simulate the cholesteatoma, according to the work of Tilleman et al.[29] that

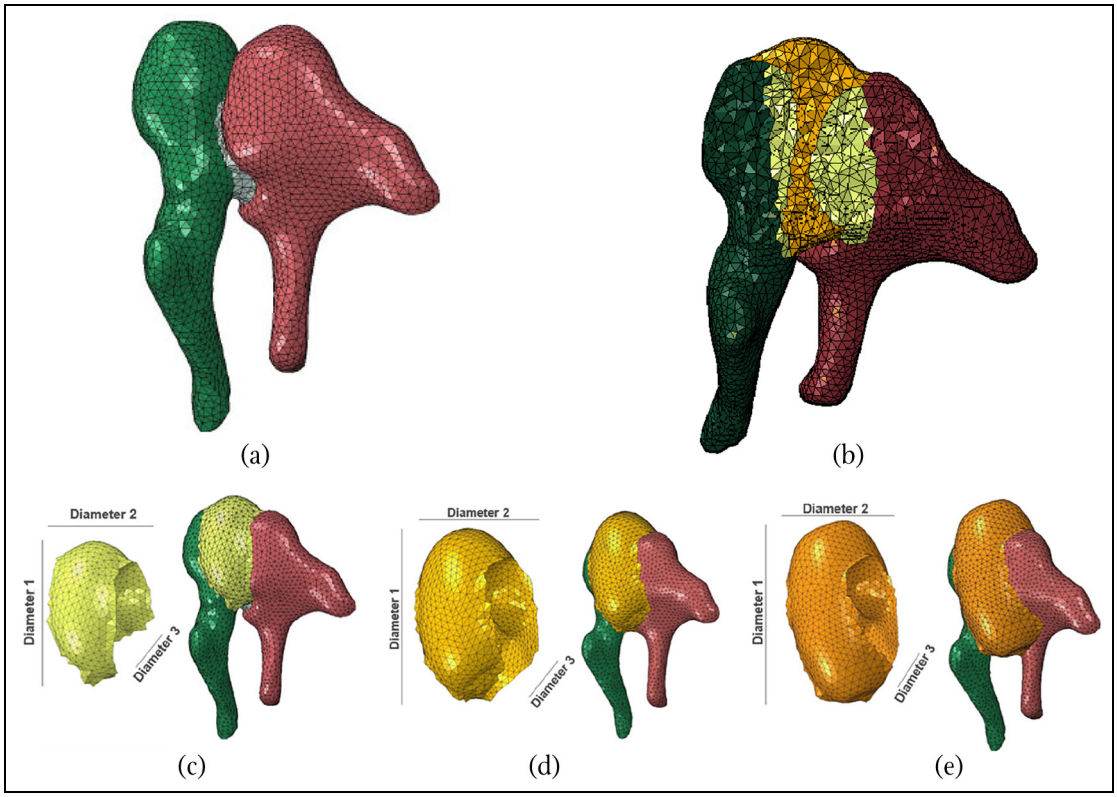

Figure 2. Simulation of cholesteatoma growth: (a) healthy state (no cholesteatoma), (b) and (c) small cholesteatoma finite element mesh in its position in the ossicular chain, (d) medium cholesteatoma mesh in its position in the ossicular chain, and (e) large cholesteatoma finite element mesh in its position in the ossicular chain.

Table 2. Dimension and mesh information of the three modeled cholesteatomas.

	Small cholesteatoma		Medium cholesteatoma		Large cholesteatoma	
	Elements	Nodes	Elements	Nodes	Elements	Nodes
Number	6556	1044	13,003	2101	17,669	2859
Type	C3D4	—	C3D4	—	C3D4	—
Diameter 1 (mm)	3.97		4.90		5.80	
Diameter 2 (mm)	2.73		3.26		3.50	
Diameter 3 (mm)	1.86		2.86		3.15	
Volume (mm^3)	5.96		13.04		19.28	

studied cancerous skin mechanical properties, this tissue Poisson's ratio is 0.43 ± 0.12 and the Young's modulus is, on average, 52 kPa. This way, an elastic behavior considering these values was defined for the created cholesteatomas. The density of the cholesteatomas was assumed as $1.2 \times 10^3\,kgm^{-3}$.

To create the cholesteatomas, their geometry was constructed and the surface mesh was generated. This mesh was then attached to the ossicles, with some of the cholesteatomas elements using malleus and incus nodes. After this, the cholesteatomas volume was filled with tetrahedral elements with 4 nodes (C3D4). Figure 2 shows the different sized cholesteatomas created and the tumor degradation that was simulated.

Once the cholesteatomas and their finite elements meshes were created and their properties defined, this data was added to the already existing model and new results were obtained. The dynamic analysis was performed according to middle ear FEM simulations from the works of Puria et al.[15] and Zhang and Gan,[30] using the simple model with the three different sized cholesteatomas, for frequencies between 100 Hz and 10 kHz and for 80 dB SPL.[26]

The displacement of both the umbo, in the central part of the TM, and the stapes footplate were analyzed for the healthy case, with no cholesteatoma, and for the three different cholesteatoma sizes. As the tympanic membrane is the first portion of the ossicular chain and

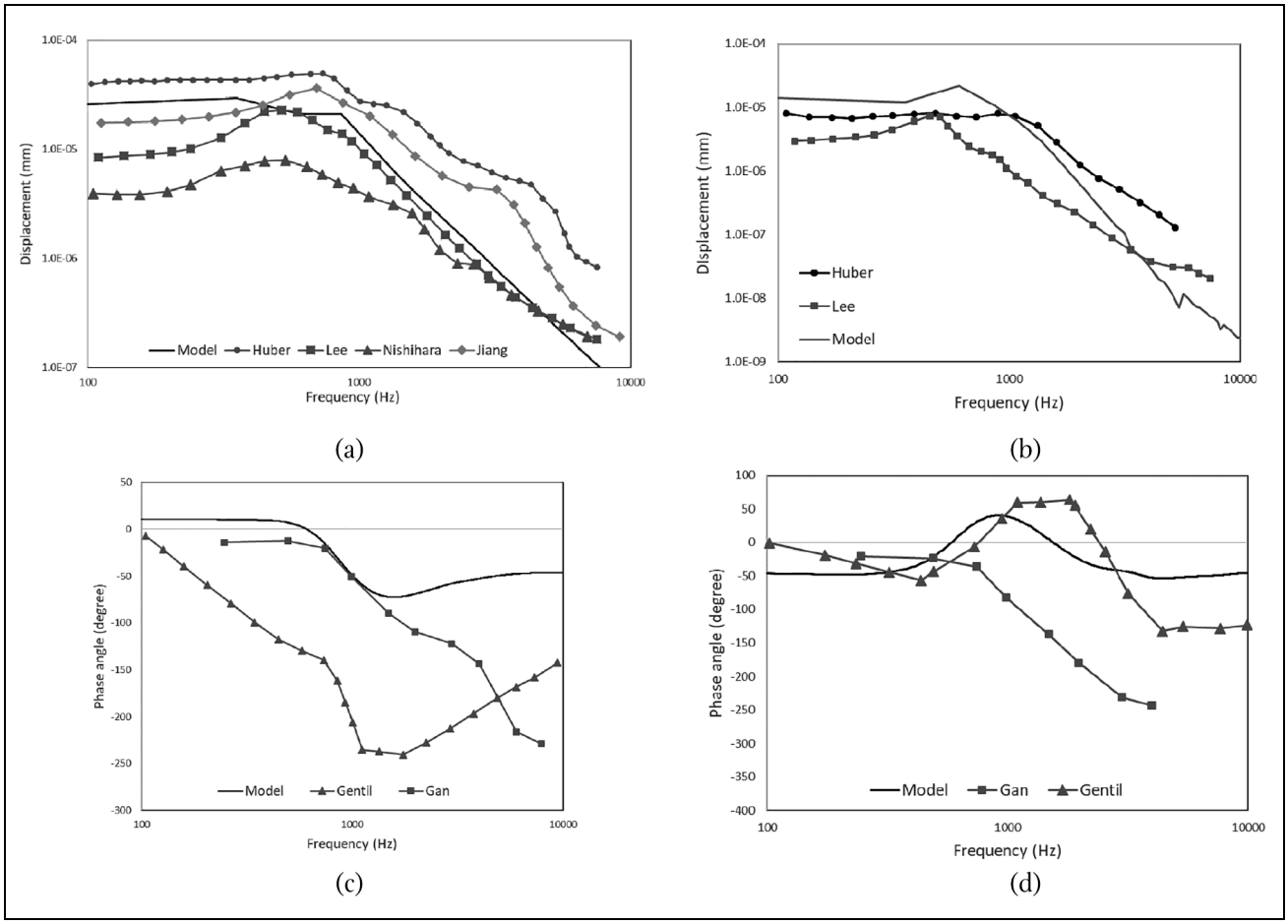

Figure 3. (a) Umbo, (b) stapes footplate displacements for 80 dB SPL, obtained by different authors, (c) umbo phase angle, and (d) stapes phase angle.

the begin of the vibratory stimulus transmission, any change in its displacement will influence the sound transmission. If the cholesteatoma could influence the tympanic membrane displacement it will affect all the sound transmission along ossicular chain until the stapes. Our aim is to understand if the cholesteatoma grow influence the ossicular chain from top to bottom.

After these first simulations, and as the cholesteatoma properties vary along their development, becoming a harder and denser structure, new simulations were performed for the larger cholesteatoma. This time, the chosen properties were similar to the ones of the ossicles, being its Young's modulus $1.41 \times 10^{10}\,\mathrm{Nm}^{-2}$, its Poisson's coefficient 0.3 and its density 2.36×10^{-9} kgm^{-3}, equal to the incus body. The simulations were conducted for the same frequencies and sound pressure level.

Finally, a simulation considering that cholesteatomas cause the degradation of the nearby structures was performed. As mentioned before, cholesteatomas are able to recruit osteoclasts, that lead to bone destruction. According to Duboeuf et al.[31] ossicles coming from ears with chronic inflammation show evidences of degradation, namely an increased porosity. In order to mimic this phenomenon, the properties of the common section between the merge of both geometries were modified to be equal to the cholesteatoma', in other words, the properties of all the elements of the ossicles' mesh wrapped by the cholesteatoma geometry. This simulation intended to mimic the replacement of the ossicles by the cholesteatoma in the regions that were degraded by the osteoclasts. This way, these ossicles' elements were selected and their properties were modified, for the three cholesteatoma sizes. Thus, their Young's modulus became 52 kPa and their Poisson's ratio 0.43, the same as the cholesteatoma's material. Once again, the simulations were performed for the same frequency band and 80 dB SPL.

Results

A dynamic study was conducted, for a frequency band between 100 Hz and 10 kHz, for 80 dB SPL, applied in the TM. Once the desired simulations were performed, the obtained results were analyzed. The steady state response was obtained, being the displacements of a node in the umbo as well as of a central node in the stapes footplate compared for the different simulated conditions, node A and B respectively in Figure 1. This way, the effect of cholesteatoma development on

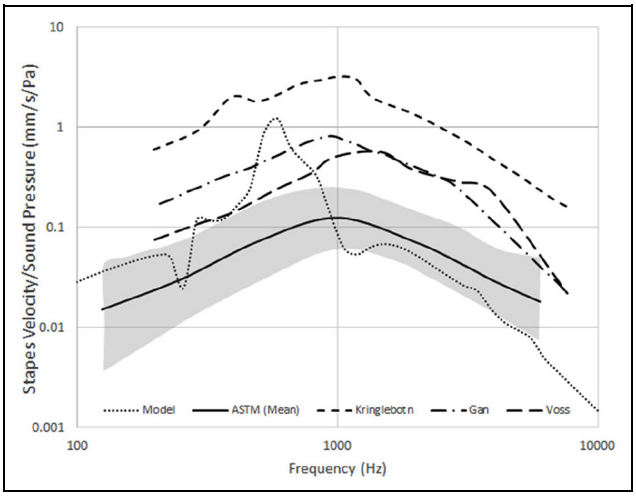

Figure 4. Magnitude of stapes velocity measurements normalized by sound pressure.

hearing was assessed before (umbo) and after (stapes footplate) sound transmission along the ossicular chain.

Initially, the obtained displacements and phase angle for the healthy case were compared with the values obtained by other authors in previous studies, in order to validate the model. These results are presented in Figure 3.

The work of Nishihara and Goode[32] is based on experimental data obtained from individuals with normal hearing. The other authors, Huber et al.,[33] Jiang et al.[34], and Lee et al.[35] studied the hearing function using a finite element model. In their research, these groups analyzed the displacement of the umbo and stapes footplate, for 80 dB SPL. The phase angle results were compared with the work of Gentil et al.[36] and Gan et al.[37]

In what concerns the umbo, the values for displacement presented by Lee et al.[35] and Nishihara and Goode[32] are slightly lower than the ones of the present model, specially for low frequencies, while the results of Huber et al.[33] are higher than the ones obtained through the used model for all the analyzed frequency band. The results of Jiang et al.[34] showed the closest results to the present model for frequencies below 400 Hz and slightly higher displacements for all high frequencies. For the stapes footplate displacements, the used model shows higher displacements for lower frequencies. Regarding the phase angle of the umbo and stapes footplate, the results are almost identical to the other authors for low frequencies (until 1000 Hz) and only deviates in the high frequencies. This differences may be explained by some differences in the model as the ligaments structures and the boundary conditions in each model or experimental work.

Figure 4 shows the comparison of the stapes velocity normalized by the ear canal pressure with other authors[14,38,39] and also including the ASTM standard for stapes motion.[40] Our model response is inside the ASTM standard average band in almost all the frequency range analyzed, which seems a closer result comparing with the other authors in the same conditions.

The modal analysis of the computational middle ear model was also performed and compared with the work of Homma et al.[41] The first natural frequency with a "rocking mode" motion was obtained at 289.4 Hz in the present model and the "pivoting mode" (second natural frequency) was obtained at 587.8 Hz. Despite the difference between the results, it could be explained by the variations in the model structures, for example, the Homma et al. work[41] does not include the superior incudal ligament, which is the ligament that connect the malleus to the roof of the tympanic cavity, influencing the motion of the ossicular chain and consequently the mode shapes of the structure as well as the natural frequencies. The boundary conditions, mesh size, and material properties are other factors that could explain the differences obtained.

Figure 5 shows the comparison for the four different scenarios, healthy ear and small, medium, and large cholesteatomas.

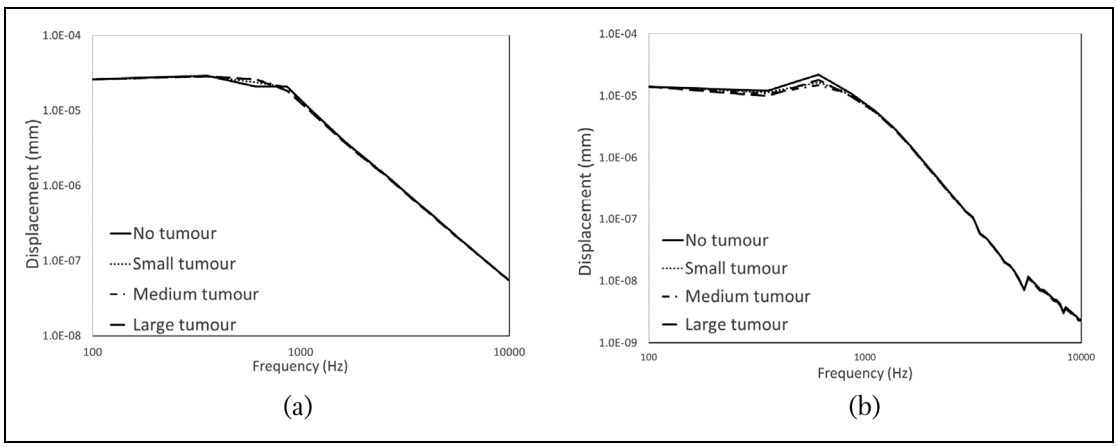

Figure 5. Umbo (a) and stapes footplate (b) displacements for healthy case and the three cholesteatoma sizes for 80 dB SPL.

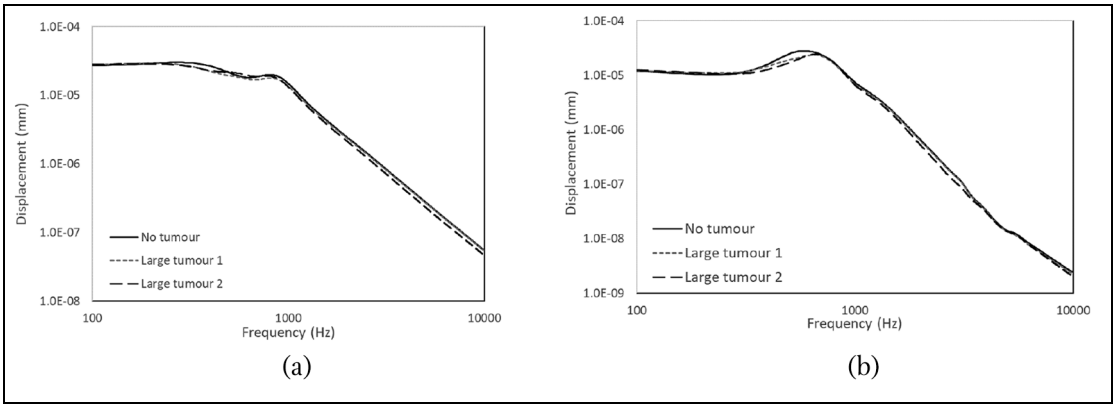

Figure 6. Umbo (a) and stapes footplate (b) displacements for healthy case and the large cholesteatoma considering normal cholesteatoma properties and cholesteatoma properties similar to the ossicles for 80 dB SPL.

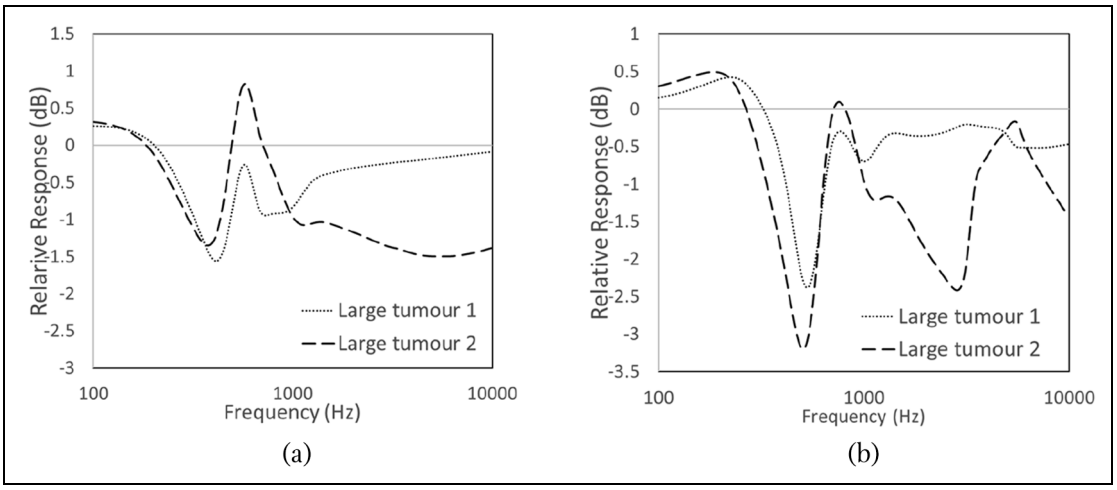

Figure 7. Umbo (a) and stapes footplate (b) relative response (dB) of large cholesteatomas to the healthy case.

Figure 5 presents the effects of cholesteatoma growth on hearing. For the umbo, the displacements are highly similar for the four cases, usually with a decrease as the cholesteatoma develops. For the stapes footplate, the values are also extremely close to each other, although there is a decrease in the displacement as the cholesteatoma appears and grows. The major difference happens, once again, for low frequencies, mainly around 600 Hz.

The following results concern the simulations with the larger cholesteatoma having properties similar to the ossicles, being shown in Figure 6. Three curves are plotted, the one related to the normal state, no cholesteatoma, the one that concerns the large cholesteatoma with the originally defined mechanical properties, large cholesteatoma 1, and the one regarding the large cholesteatoma with properties similar to the ossicles and large cholesteatoma 2. The difference in what concerns the displacements is more visible through the relative response (dB) of the larges cholesteatomas to the healthy case in Figure 7.

As we are working on tiny scales, a relative response (in dB) is presented in the Figure 7 to enhance the analysis. For all the analyzed frequency band it is possible to see slightly differences for the cholesteatoma with properties similar to the ossicles in comparison to the initial cholesteatoma stage with softer properties mainly for low frequencies. In the case of the stapes footplate response, it shows higher hearing loss in the case of the cholesteatoma with bony properties for high frequencies from 1000 to 3000 Hz.

The next simulation was the one that considered ossicles degradation. This simulation resembles better to the real scenario, where cholesteatomas have the ability to recruit osteoclasts due to the inflammatory reaction they trigger, and degrade the ossicles. This way, Figures 8 to 10, that concern the small, medium, and large cholesteatomas, respectively, show the results of the simulations including bone degradation. In these tests, the mechanical properties of the ossicles' elements that were wrapped by the cholesteatoma (incudomalleolar joint and part of the malleus and the incus) were

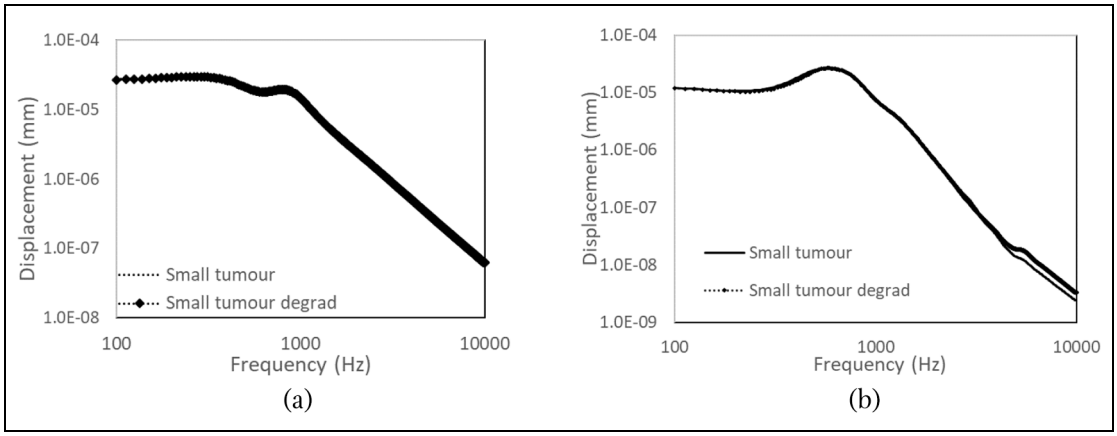

Figure 8. Umbo (a) and stapes footplate (b) displacements for the small cholesteatoma considering normal ossicles properties and cholesteatoma degradation, for 80 dB SPL.

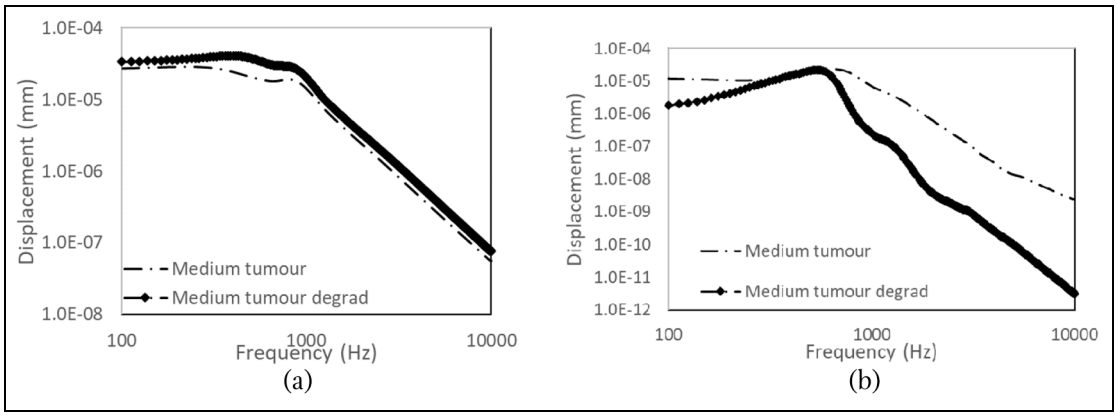

Figure 9. Umbo (a) and stapes footplate (b) displacements for the medium cholesteatoma considering normal ossicles properties and cholesteatoma degradation, for 80 dB SPL.

modified to have the same properties as the cholesteatoma. In these graphs, the displacements for the umbo and the stapes footplate for 80 dB SPL are presented for the different cholesteatoma sizes. The results are compared between each cholesteatoma, for the case in which ossicle degradation is not considered and for the degradation simulation.

Regarding the results for the small cholesteatoma, the displacement differences between both conditions in the umbo and stapes show few variation as expected, as the small cholesteatoma degrade a minimal portion of the bones that does not seems to have impact in the sound transmission.

For the medium and large cholesteatomas the differences are higher than the small cholesteatoma. The results showed slightly higher displacements in umbo when the ossicles degradation were considered for all the frequency band and lower displacements in the stapes (Figures 9 and 10). The higher umbo displacement in the degradation case might be explained by the fact that the ossicular chain becomes softer and less dense when degradation is considered and so it offers less resistance to vibrations, leading to around 50% higher displacement of the umbo, with 10% difference between the medium and large cholesteatoma, with higher differences for the large structure.

On the other hand, the stapes footplate displacements are generally lower for the case where degradation is considered for both the medium and large cholesteatoma simulations, which was expected as a softer material will not favor the transmission of sound information. Besides the small differences in the medium cholesteatoma for low frequencies; from 1000 to 10000 Hz (high frequencies), the stapes footplate displacement in the case of ossicles degradation for medium and large cholesteatoma is around 10^4 times smaller.

Additionally, Figure 11 shows the change in the response in dB obtained for the ossicles degradation case for all the cholesteatoma sizes relative to the healthy condition simulation in order to improve the results analysis.

Regarding the results for the small cholesteatoma, the relative response registered in the umbo and stapes

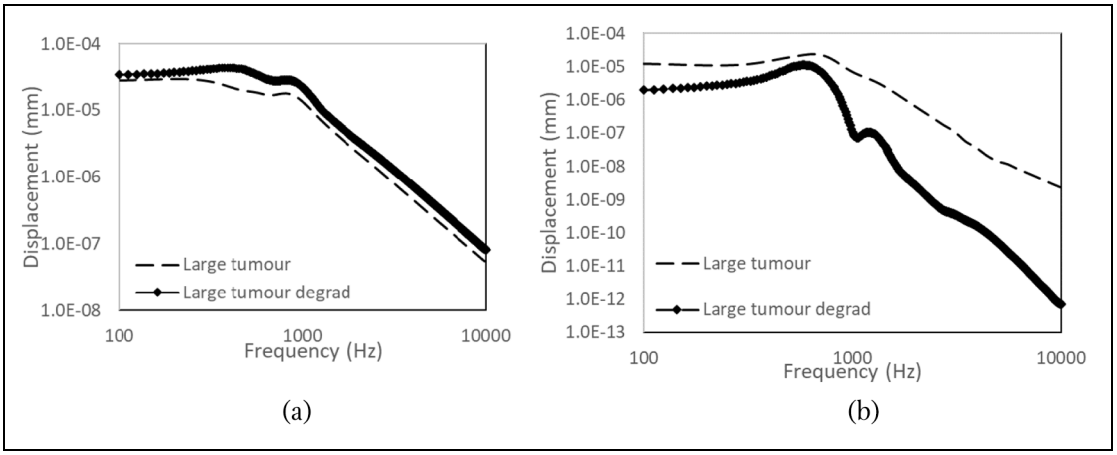

Figure 10. Umbo (a) and stapes footplate (b) displacements for the large cholesteatoma considering normal ossicles properties and cholesteatoma degradation, for 80 dB SPL.

for ossicles degradation showed few variation as expected. Despite the difference starts to increase from 1000 to 10000 Hz in the umbo for the small cholesteatoma, this is not identified in the stapes response, which could not be translated to hearing loss. The slightly impact of the ossicles' degradation in the umbo response for the medium and large cholesteatoma could be related to the changes in the material chain near the tympanic membrane. The stapes response showed severe differences in hearing loss from 10 to 20 dB in degradation condition of the medium and large cholesteatomas for low frequencies (100–1000 Hz) and an average loss of 50.08 dB for high frequencies (1000–10000 Hz).

Discussion

Through the results presented in Figures 3 and 4 it is possible to observe that the computational model used in the present work has a similar behavior to other biomechanical models of the ear and experimental data mainly for stapes velocity and umbo and stapes displacement, as the phase angle results slightly deviates in the higher frequencies. The observed differences may be due to the discrepancy between some of the modeled structures values and dimensions regarding the literature values.

In the analysis of cholesteatoma growth (Figure 5) it is possible to observe that the major difference happens around 600 Hz, where the healthy case is associated to the lowest displacement value, which goes against what happens for the majority of frequencies, where the case without cholesteatoma has the higher displacement value. Therefore, this point was disregarded for not conveying relevant information. As the small cholesteatoma is still in its initial stage of development, it is not likely to trigger any symptoms. This way, the fact that its dimensions are not among the values described in literature is acceptable.

The values obtained for the stapes footplate are more relevant than the ones obtained for the umbo, as the stapes footplate is located at the end of the ossicular chain, after sound being transmitted through the ossicles, where the cholesteatoma is placed. The stapes footplate displacements allow to understand the amount of sound information that will proceed to the inner ear and, so, reach the brain. Despite the influence of the cholesteatoma will have greater impact in the stapes than in the umbo, the cholesteatoma is placed near the umbo in the present study, which could also influence the sound transmission from the chain entry. Our aim is to understand if the cholesteatoma grow influence the ossicular chain from top to bottom.

It is important to underline that these first simulations intended to study the influence of cholesteatoma presence and its growth, having the three cholesteatomas the same properties and not including any effect on the ossicles. These simulations are far from real life conditions. Nevertheless, they were considered useful as a first approach to study damping phenomena due to cholesteatoma development in the middle ear.

The results presented in Figure 6 are related with the simulations with different cholesteatoma properties. As the cholesteatoma with properties similar to the ossicles (Figures 6 and 7) could be considered an immobilized joint (incudomalleolar joint (IMJ)), and perhaps the different sound pressure used, the work of Gerig et al.[42] also showed higher differences in translational motion of stapes in the case of immobilized IMJ compared with normal IMJ from 1500 to 6000 Hz.

This data sustains the idea that the cholesteatoma properties evolve along time, as people with cholesteatoma sometimes realize they have this condition when they start to experience hearing loss, so the difference in terms of stapes footplate displacement should be higher than the ones plotted in Figure 5. Further studies exploring different properties, that confer different behavior to the cholesteatoma, transforming it in a

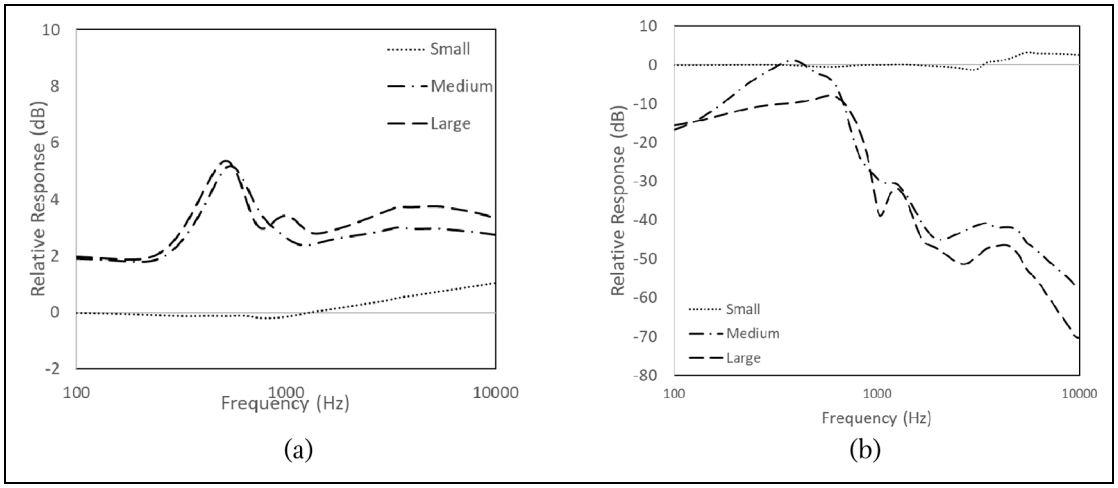

Figure 11. Umbo (a) and stapes footplate (b) relative response (dB) of cholesteatoma degradation to the normal healthy situation (without cholesteatoma).

harder and denser structure but having properties that not the ossicles' would be of interest.

Finally, the results related to the simulation considering the ossicles degradation were analyzed. Figure 11 shows the relative response in dB between the ossicles degradation and the healthy condition (without cholesteatoma) in order to clear the analysis.

The results showed a residual difference in the case of the small cholesteatoma as expect, since the small cholesteatoma does not seems to have a role in hearing loss. Despite the lack of consensus regarding the influence of a cholesteatoma in hearing loss among scientific community, the degradation of the ossicular chain seems to be frequent. Some level of ossicular degradation was found in more than 90% of the 80 cases analyzed in the work of Olsen et al.[43] and around 83% in the 100 patients studied in the work of Khdim et al.[10]

One of the most recent works[10] that compare hearing loss in different cholesteatoma conditions showed an average loss of 54.1 dB in 80% of the evaluated cases, with the cholesteatoma placed in the antro attical location. Our results seem to be according with the ones obtained from Olsen et al.[43] which found an average loss of 50.86 (air threshold) and 50.34 dB for 2000 and 4000 Hz, respectively, in a secondary cholesteatoma. In Figure 11 we can see and average of 49.0 dB loss for the large cholesteatoma between the same range from 2000 to 4000 Hz, which is a close results comparing with the experimental values of the Olsen et al.[43] research. The main difference is regarding the low frequencies between 500 and 1000 Hz where our results showed an average hearing loss of 16.01 dB for the large cholesteatoma, while the Olsen et al.[43] research present the same 50 dB loss for low frequencies.

Several factors as the cholesteatoma size and location could influence the obtained results and should be considered in further future analysis of experimental and computational research.

Conclusion

The obtained results suggest that the sound information that proceeds to the inner ear decreases as the cholesteatoma appears and grows in the middle ear. The fact that the cholesteatoma properties evolve along time contribute to higher damping phenomena, resulting in even less information reaching the stapes. When ossicles degradation is considered, there is a higher variation in the results, keeping the trend of hampering hearing. In the current work, the performed analysis simulated that the cholesteatoma had the ability to degrade the ossicles and completely replace the degraded portions. Nevertheless, an intermediate simulation, in which only some portions of the ossicles would be altered instead of all the part of the ossicles involved by the cholesteatoma, would be of interest, so several degrees of degradation could be studied. Furthermore, as the osteoclasts activity completely degrades the ossicles, it is possible that the degraded parts are not replaced by the cholesteatoma. In this case, the ossicular chain could be interrupted, which would lead to severe conductive hearing loss. A simulation of this condition, where some parts of the ossicles would be removed to better reproduce osteoclasts activity would also be interesting. Additionally, an analysis in which cholesteatoma growth could be mimicked in a more accurate way instead of only three cholesteatoma sizes would provide more information.

Declaration of conflicting interests

The author(s) declared no potential conflicts of interest with respect to the research, authorship, and/or publication of this article.

Funding

The author(s) disclosed receipt of the following financial support for the research, authorship, and/or

publication of this article: The authors acknowledge the funding by Ministério da Ciência, Tecnologia e Ensino Superior through Portuguese Foundation for Science and Technology (FCT) under research grant SFRH/BD/108292/2015. Additionally, the authors gratefully acknowledge the funding of Project UIDB/50022/2020—cofinanced by LAETA and FCT.

ORCID iDs

Carla F. Santos https://orcid.org/0000-0002-0304-1356
Fernanda Gentil https://orcid.org/0000-0002-6521-3475

References

1. Zahnert T. Differenzialdiagnose der schwerhörigkeit. *Dtsch Arztebl* 2011; 108(25): 433–444.
2. Morris PS and Leach AJ. Acute and chronic otitis media. *Pediatr Clin North Am* 2009; 56(6): 1383–1399.
3. World Health Organization. *Chronic suppurative otitis media: burden of illness and management options*. Geneva: WHO, 2004.
4. World Health Organization. *Global costs of unaddressed hearing loss and cost-effectiveness of interventions a WHO report, 2017*. Geneva: WHO, 2017.
5. Ikeda M, Nakazato H, Onoda K, et al. Facial nerve paralysis caused by middle ear cholesteatoma and effects of surgical intervention. *Acta Otolaryngol* 2006; 126(1): 95–100.
6. Kennedy KL and Singh AK. *Middle ear cholesteatoma*. Treasure Island, FL: StatPearls Publishing, 2020.
7. Lips LMJ, Nelemans PJ, Theunissen FMD, et al. The diagnostic accuracy of 1.5 T versus 3 T non-echo-planar diffusion – weighted imaging in the detection of residual or recurrent cholesteatoma in the middle ear and mastoid. *J Neuroradiol* 2020; 47(6): 433–440.
8. Chang P and Kim S. Cholesteatoma – diagnosing the unsafe ear. *Aust Fam Physician* 2008; 37(8): 631–638.
9. Mankowski NL and Raggio BS. *Otoscope exam*. Treasure Island, FL: StatPearls Publishing, 2020.
10. Khdim M, Douimi L, Choukry K, et al. Hearing loss in cholesteatoma. *J Otolaryngol Head Neck Surg* 2020; 3(8): 1115.
11. Bhutta MF, Williamson IG and Sudhoff HH. Cholesteatoma. *BMJ* 2011; 342: d1088.
12. Wang H, Northrop C, Burgess B, et al. Three-dimensional virtual model of the human temporal bone. *Otol Neurotol* 2006; 27(4): 452–457.
13. Gan RZ, Sun Q, Feng B, et al. Acoustic-structural coupled finite element analysis for sound transmission in human ear – pressure distributions. *Med Eng Phys* 2006; 28(5): 395–404.
14. Gan RZ, Reeves BP and Wang X. Modeling of sound transmission from ear canal to cochlea. *Ann Biomed Eng* 2007; 35(12): 2180–2195.
15. Puria S. Measurements of human middle ear forward and reverse acoustics: implications for otoacoustic emissions. *J Acoust Soc Am* 2003; 113(5): 2773–2789.
16. O'Connor 16, Cai H and Puria S. The effects of varying tympanic-membrane material properties on human middle-ear sound transmission in a three-dimensional finite-element model. *J Acoust Soc Am* 2017; 142(5): 2836–2853.
17. Gentil F, Parente M, Martins P, et al. Effects of the fibers distribution in the human eardrum: a biomechanical study. *J Biomech* 2016; 49(9): 1518–1523.
18. Berdich K, Gentil F, Parente M, et al. Finite element analysis of the transfer of sound in the myringosclerotic ear. *Comput Methods Biomech Biomed Engin* 2016; 19(3): 248–256.
19. Liu H, Zhang H, Yang J, et al. Influence of ossicular chain malformation on the performance of round-window stimulation: a finite element approach. *Proc Inst Mech Eng H* 2019; 233(5): 584–594.
20. Areias B, Santos C, Natal Jorge RM, et al. Finite element modelling of sound transmission from outer to inner ear. *Proc Inst Mech Eng H* 2016; 230(11): 999–1007.
21. Sørensen MS, Dobrzeniecki AB, Larsen P, et al. The visible ear: a digital image library of the temporal bone. *ORL J Otorhinolaryngol Relat Spec* 2002; 64(6): 378–381.
22. Abaqus CAE. *Finite element analysis*. ABAQUS Inc, 2018. Dassault Systèmes Simulia Corp.
23. Sun Q, Gan RZ, Chang KH, et al. Computer-integrated finite element modeling of human middle ear. *Biomech Model Mechanobiol* 2002; 1(2): 109–122.
24. De Greef D, Pires F and Dirckx JJJ. Effects of model definitions and parameter values in finite element modeling of human middle ear mechanics. *Hear Res* 2017; 344: 195–206.
25. Muyshondt PGG and Dirckx JJJ. Structural stiffening in the human middle ear due to static pressure: finite-element analysis of combined static and dynamic middle-ear behavior. *Hear Res* 2021; 400: 108116.
26. André Faria Areias B. *Simulação Biomecânica Do Ouvido Humano, Incluindo Patologias Do Ouvido Médio*. Faculty of Engineering of the University of Porto, Portugal. 2014.
27. Holm KB. *The chorda tympani nerve: role in taste impairment in middle ear disease and after ear surgery*. Faculty of Medicine, Uppsala University, Sweden. 2017.
28. Goyal A, Singh PP and Dash G. Chorda tympani in chronic inflammatory middle ear disease. *Otolaryngol Head Neck Surg* 2009; 140(5): 682–686.
29. Tilleman TR, Tilleman MM and Neumann MHA. The elastic properties of cancerous skin: Poisson's ratio and Young's modulus. *Isr Med Assoc J* 2004; 6(12): 753–755.
30. Zhang X and Gan RZ. Finite element modeling of energy absorbance in normal and disordered human ears. *Hear Res* 2013; 301: 146–155.
31. Duboeuf F, Burt-Pichat B, Farlay D, et al. Bone quality and biomechanical function: a lesson from human ossicles. *Bone* 2015; 73: 105–110.
32. Nishihara S and Goode RL. Measurement of tympanic membrane vibration in 99 human ears. In: Hüttenbrink K-B (ed.) *Middle ear mechanics in research and otosurgery*. Dresden, Germany: Department of Oto-Rhino-Laryngology, Dresden University of Technology, 1997, pp.91–93.
33. Huber A, Ball G, Asai M, et al. *The vibration pattern of the tympanic membrane after placement of a total ossicular replacement prosthesis (TORP)*. Dresden, Germany: Department of Oto-Rhino-Laryngology, Dresden University of Technology, 1997.
34. Jiang XP, Li CH, Ding H, et al. Influence of different materials for artificial auditory ossicle on the dynamic characteristics of human ear and research on hearing recovery. *J Vibroengineering* 2017; 19(4): 2995–3007.

35. Lee CF, Chen PR, Lee WJ, et al. Computer aided three-dimensional reconstruction and modeling of middle ear biomechanics by high-resolution computed tomography and finite element analysis. *Biomed Eng Appl Basis Commun* 2006; 18(5): 214–221.
36. Gentil F, Garbe C, Parente M, et al. The biomechanical effects of stapes replacement by prostheses on the tympano-ossicular chain. *Int J Numer Method Biomed Eng* 2014; 30(12): 1409–1420.
37. Gan RZ, Wood MW and Dormer KJ. Human middle ear transfer function measured by double laser interferometry system. *Otol Neurotol* 2004; 25(4): 423–435.
38. Voss SE, Rosowski JJ, Merchant SN, et al. Acoustic responses of the human middle ear. *Hear Res* 2000; 150(1–2): 43–69.
39. Kringlebotn M. Network model for the human middle ear. *Scand Audiol* 2009; 17(2): 75–85.
40. ASTM International. *Standard specification and test methods for metallic bone staples*. ASTM F564-17, 2017. West Conshohocken, PA: ASTM International, https://www.astm.org/Standards/F564.htm (accessed 21May, 2021).
41. Homma K, Du Y, Shimizu Y, et al. Ossicular resonance modes of the human middle ear for bone and air conduction. *J Acoust Soc Am* 2009; 125(2): 968–979.
42. Gerig R, Ihrle S, Röösli C, et al. Contribution of the incudo-malleolar joint to middle-ear sound transmission. *Hear Res* 2015; 327: 218–226.
43. Olsen JM, Ribeiro Fde A, Yasui MM, et al. Hearing loss assessment in primary and secondary acquired cholesteatoma. *Braz J Otorhinolaryngol* 2015; 81(6): 653–657.